Interpreting the effect of operating variable, seed, and impurity on the induction time of silver nanoparticles precipitation by cluster coagulation models

Negin Hatami, Sattar Ghader*

Department of Chemical Engineering, College of Engineering, Shahid Bahonar University of Kerman, Jomhoori Blvd., Kerman, Iran

HIGHLIGHTS

- The effects of temperature, impurity (Fe^{3+}) and crystal seed on the induction time of silver nanoparticles is investigated.

- Experimental induction time was compared to the cluster coagulation models.

- The presence of Fe^{3+} prolongs the induction time.

- The Cluster model is overly simplified and does not properly model precipitation process.

GRAPHICAL ABSTRACT
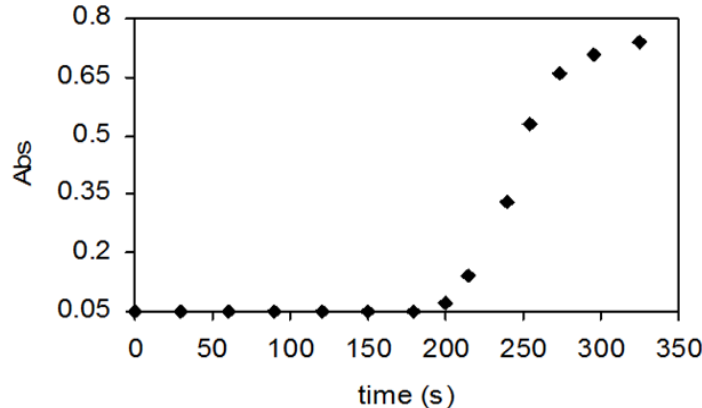
ABSTRACT

This paper reports the effect of temperature, presence of impurity (Fe^{3+}), and crystal seed on the induction time of silver nanoparticles. In this study, Ag precipitation was achieved by solution reduction and the experimental induction time was measured by monitoring the absorption of the solution after creation of supersaturation. Experimental induction time was compared to the cluster coagulation models (the Smoluchowski model and its' variation cluster coagulation model) and the conclusion is that the conventional Smoluchowski coagulation model works better than the modified version.

1. Introduction

Induction time, t_{ind}, is defined as the time that elapses between the creation of supersaturation and the formation of critical nuclei. Induction time is considered as being made up of several parts. For example, a certain 'relaxation time', t_r, is required for this system to achieve a quasi-steady state distribution of molecular clusters. Time is also required for the formation of a stable nucleus, t_n, and then for the nucleus to grow to a detectable size, t_g. Thus, the induction time may be written [1]:

$$t_{ind} = t_r + t_n + t_g \tag{1}$$

In a low-viscous aqueous solution of an electrolyte, the relaxation time may be very short. So the induction time can be expressed as:

$$t_{ind} = t_n + t_g \tag{2}$$

Induction time cannot be regarded as a fundamental property of crystallization since its value depends on the method used to detect the formed crystals. Induction time is inversely related to the nucleation rate, and hence depends on supersaturation, temperature and interfacial tension, etc. [1,2]. Induction time is also influenced by external factors such as the presence of impurities and crystal seed. Nevertheless, the induction time is experimentally accessible and contains information about the kinetics of new phase nucleation [2].

Recently, the synthesis and study of silver nanoparticles has achieved great attention both in research and technology [3-6]. Theoretical modeling of induction time in precipitation of nanoparticles is in early stages and even existing models for induction time have not been applied to nanoparticle crystallization. In this study, the induction time of silver nanoparticles is determined experimentally and compared with the predictions of two models, Smoluchowski's coagulation theory and cluster coagulation model [7,8].

2. Theoretical background

2.1. Smoluchowski's coagulation theory

Suppose that the collision of two clusters yields a larger cluster containing the sum of the entities in each,

and the breakup of a large cluster yields two smaller ones. Then, the temporal variation in cluster size distribution can be described by Smoluchowski's coagulation theory [7]:

$$\frac{dC_n}{dt} = \frac{1}{2} \sum_{k=1}^{n-1} \left[a_{n-k,k} C_{n-k} C_k - b_{n-k,k} C_n \right] - \sum_{k=1}^{\infty} \left[a_{nk} C_n C_k - b_{nk} C_{n+k} \right] \tag{3}$$

where C_n is the concentration of clusters of size n (n-mer), a_{ij} is the association coefficient between clusters of sizes i (i-mer) and j (j-mer), b_{ij} is the dissociation coefficient of clusters of size $(i+j)$, and t denotes time. Here, a_{ij} measures the rate of formation of clusters of size $(i+j)$ through association of clusters of sizes i and j, and b_{ij} determines the rate of formation of clusters of size i (or j) through breakup of clusters of size $(i+j)$. If $b_{ij} = 0$, it can be shown that Eq. (3) can be solved analytically for the following three special cases [7]:

$$\text{Case 1: } a_{ij} = K_1 \tag{4a}$$

$$\text{Case 2: } a_{ij} = K_2 \, (i+j) \tag{4b}$$

$$\text{Case 3: } a_{ij} = K_3 \, ij \tag{4c}$$

In these expressions K_1, K_2 and K_3 are constants. Eq. (4a) implies that the rate of formation of a cluster is independent of the sizes of its precursors. Eq. (4b) suggests that the rate of formation of a cluster is proportional to the sum of the sizes of its precursors, and Eq. (4c) states that the rate of formation of a cluster is proportional to the product of the sizes of its precursors. The temporal variation in mean cluster size $\bar{n}$, can be derived according to Eqs. (4a) - (4c) [7]:

$$\text{Case 1: } \quad \bar{n} = 1 + \frac{K_1 C_0 t}{2} \tag{5a}$$

$$\text{Case 2: } \quad \bar{n} = exp \, (K_2 C_0 t) \tag{5b}$$

$$\text{Case 3: } \quad \bar{n} = \frac{2}{2 - K_3 C_0 t} \tag{5c}$$

where C_0 denotes the initial concentration of monomers. According to the classical theory of homogeneous nucleation, when a solution is supersaturated the monomers in solution start to coagulate and then form clusters. If the size of a cluster exceeds a critical size g_c, a

critical nucleus is born, and its subsequent growth leads to a crystal. The critical cluster size can be estimated by employing the thermodynamics arguments, and was derived by [8]:

$$g_c = \frac{32\pi V_m^2 \delta^3}{3(kT \ln S)^3} \tag{6}$$

In this expression, V_m is the volume of a monomer, δ is the interfacial tension of crystal, k is the Boltzmann constant, T is the temperature, and S is the degree of supersaturation. We assume that when the mean cluster size in a solution reaches the critical cluster size the primary nucleation occurs spontaneously. The time at which reaches gc is defined as the induction time tind. If we let $\bar{n} = g_c$ and $t = t_{ind}$ in Eqs. (5a)-(5c) and solve the resultant expressions for t_{ind}, we obtain:

$$\text{Case 1:} \quad t_{ind} = \frac{2}{K_1 C_0}(g_c - 1) \tag{7a}$$

$$\text{Case 2:} \quad t_{ind} = \frac{1}{K_2 C_0} \ln(g_c) \tag{7b}$$

$$\text{Case 3:} \quad t_{ind} = \frac{2}{K_3 C_0}\left(1 - \frac{1}{g_c}\right) \tag{7c}$$

These expressions, together with Eq. (6), provide the formulae for calculation of induction time.

The introduction of crystal seed will accelerate the rate of crystal growth. Due to van der Waals attractive force, the concentration of clusters near the surface of a seed is higher than that in the bulk liquid phase; therefore, the rate of association between clusters is accelerated. It can be shown that the concentration of spherical monomers of radius r_1 at a distance d from seed surface C'_0 is [7]:

$$C'_0 = C_0 \exp\left(\frac{A r_1}{6kTd}\right) \tag{8}$$

where C_0 is the bulk concentration of monomers, d is distance from crystal surface and A is the Hamaker constant. The induction time for this case, when crystal seed are present, can be estimated by replacing C_0 with C'_0 in Eqs. (7a)-(7c) and we have:

$$\text{Case 1:} \quad t_{ind} = \frac{2}{K_1 C'_0}(g_c - 1) \tag{9a}$$

$$\text{Case 2:} \quad t_{ind} = \frac{1}{K_2 C'_0} \ln(g_c) \tag{9b}$$

$$\text{Case 3:} \quad t_{ind} = \frac{2}{K_3 C'_0}\left(1 - \frac{1}{g_c}\right) \tag{9c}$$

2.2. Cluster coagulation model

The change of cluster size distribution with time can be described by Smoluchowski's coagulation theory. However, since the rate constants for the coagulation between clusters of various sizes and the corresponding mechanism are both unknowns, evaluation of the cluster size distribution becomes nontrivial. This problem is circumvented by considering the mean or averaged behavior of the system. It was assumed that only the $\bar{g}$-mers are present initially, and they coagulate to form $2\bar{g}$-mers. Then the $2\bar{g}$-mers coagulate to give $4\bar{g}$-mers, and so on, until the critical nuclei, i.e., g_c-mers, are formed. $\bar{g}$ is the dominating size of clusters in the solution. According to this simplified model, the tind can be evaluated by the following correlation composed of three important terms related to diffusivity, coagulation concentration, and critical nuclei size [10]:

$$t_{ind} = \left(\frac{1}{8\pi D r_{\bar{g}}}\right)\left(\frac{1}{n_{\bar{g}}}\right)\left(\frac{g_c}{\bar{g}} - 1\right) \tag{10}$$

where $n_{\bar{g}}$ is the number concentration of $\bar{g}$-mers in the liquid phase. Substituting $D = \frac{kT}{6\pi\eta r_{\bar{g}}}$ into Eq. (10), we obtain:

$$t_{ind} = \left(\frac{3\eta}{4kT}\right)\left(\frac{1}{n_{\bar{g}}}\right)\left(\frac{g_c}{\bar{g}} - 1\right) \tag{11}$$

In these expression, D is the diffusivity of clusters, $\bar{g}$ is the dominating size of clusters, $r_{\bar{g}}$ is the radius of $\bar{g}$-mers, η is the viscosity of the liquid phase, k is the Boltzmann constant, and T is the temperature. $n_{\bar{g}}$ can be evaluated by:

$$n_{\bar{g}} = n_1 \exp\left(\frac{-\Delta G_{\bar{g}}}{kT}\right) \tag{12}$$

where

$$\Delta G_{\bar{g}} = \delta \sqrt[3]{4\pi\left(3\bar{g}V_m\right)^2} - \bar{g}kT \ln(S) \tag{13}$$

where n_1 is the number concentration of monomer and $\Delta G_{\bar{g}}$ is the total excess free energy for the formation of a $\bar{g}$-mers, δ and V_m are the interfacial tension of the crystal and the volume of a monomer, respectively. Substituting Eqs. (6), (12), and (13) into Eq. (11) gives:

$$t_{ind} = \left(\frac{3\eta}{4n_1 kT} \right) \tag{14}$$

$$exp\left[-\bar{g}\ln(S) + \frac{\delta\sqrt[3]{4\pi(3\bar{g}V_m)^2}}{kT} \right]\left[\frac{32\pi V_m^2 \delta^3}{3\bar{g}(kT\ln(S))^3} - 1 \right]$$

The three main terms in Eq. (14) are related to diffusivity, coagulation concentration, and critical nuclei size.

When the seed crystal is introduced into the supersaturated solution, the clusters are attracted by the van der Waals field of the seed crystal. Considering the van der Waals attractive energy between the cluster and seed crystal, the concentration of $\bar{g}$-mers at distance d from the crystal surface, $n'_{\bar{g}}$, relative to its concentration in the bulk solution, $n_{\bar{g}}$, is given by [10]:

$$n'_{\bar{g}} = n_{\bar{g}}exp\left[\frac{Ar_1}{6kTd\sqrt[3]{g}} \right] \tag{15}$$

The induction time of the seeded solution can be estimated by replacing $n_{\bar{g}}$ with $n'_{\bar{g}}$ in Eq. (11).

$$t_{ind} = \left(\frac{3\eta}{4kT} \right)\left(\frac{1}{n'_{\bar{g}}} \right)\left(\frac{g_c}{g} - 1 \right) \tag{16}$$

Substituting Eqs. (6) (13), and (15) into Eq. (16) gives:

$$t_{ind} = \left(\frac{3\eta}{4n_1 kT} \right) \tag{17}$$

$$exp\left[-\bar{g}\ln(S) + \frac{\delta\sqrt[3]{4\pi(3\bar{g}V_m)^2}}{kT} - \frac{Ar_1}{6kTd\sqrt[3]{g}} \right]\left[\frac{32\pi V_m^2 \delta^3}{3\bar{g}(kT\ln(S))^3} - 1 \right]$$

3. Experimental

3.1. Procedure

Preparation of silver nanoparticles generally involves the reduction of metal ions in a solution and without the protection of a stabilizing agent on their surface these nanoparticles undergo aggregation. The experiments were performed in a 250 mL vessel stirred by a magnetic bar at constant speed. The experimental procedures are described briefly below. A 100 mL solution of silver nitrate was made with different concentrations of 2×10^{-4}, 5×10^{-4}, 7×10^{-4}, 1×10^{-3}, 2×10^{-3} and 3×10^{-3} M , and 5 mL sodium citrate 0.034 M was added to stabilize the nanoparticles. After the solution temperature stabilized (at three levels 25, 35 and 45 ℃), 5 mL of 0.001 mol/L hydrazine hydrate was added to the vessel dropwise to

reduce the silver ions by the reaction:

$$4Ag^+ + N_2H_4.H_2O \rightarrow 4Ag + N_2 + 4H^+ \tag{18}$$

Silver nanoparticles are produced after a few minutes and the solution turns a yellow color.

The procedure for investigating the impurity effect is the sameas above except that 5 mL aqueous Fe^{3+} solution was added into the previous solution before the addition of 5 mL of 0.001 M hydrazine hydrate.

In the crystal seed experimental section, silver seeds are made by adding an excess of the reducing agent, sodium borohydride, to the silver nitrate solution:

$$Ag^+ + NaBH_4 \rightarrow Ag + \frac{1}{2}H_2 + \frac{1}{2}B_2H_6 \tag{19}$$
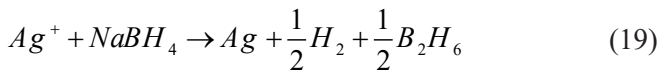
A 150 mL solution of sodium borohydride with a concentration of 0.0002 M was placed in an ice bath for 20 minutes and then 5 mL sodium citrate 0.034 M was added to this solution. Afterwards, the solution's vessel was stirred by a magnetic bar at a constant speed and then 50 mL silver nitrate with a concentration of 0.0001 M was added to the solution vessel drop wise to form crystal seeds of about 10-14 nm in diameter.

3.2. Induction time measurement

When a beam of light is directed at a nanoparticle solution some of the light may be absorbed (color is produced when light of a certain wavelength is selectively absorbed), some is scattered, and the remainder is transmitted undisturbed through the sample [11]. In the presence of a nanoparticles solution, the measured attenuation of light of intensity   in a spectrophotometer is given by [12]:

$$\frac{dI(x)}{dx} = NC_{ext}I(x) \tag{20}$$

C_{ext} is the extinction cross section of a single particle. This shows that the rate of loss of photons is proportional to the light intensity I at distance x and the number of nanoparticles per unit volume N. Integration gives the solution absorbance:

$$A = \log\left(\frac{I_0}{I(x)} \right) = \frac{NC_{ext}x}{2.303} \tag{21}$$

Therefore, induction time can be determined by monitoring the absorption of solution after creation
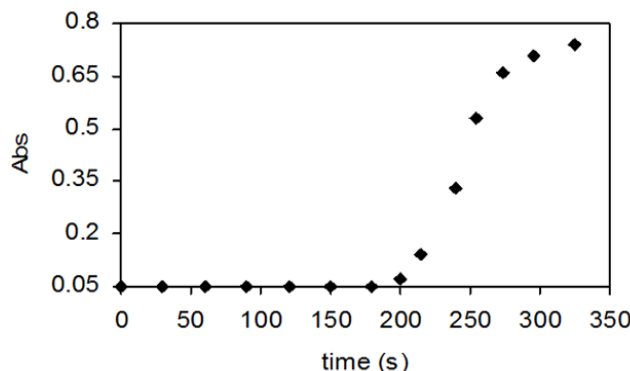
of supersaturation for all cases: precipitation of silver nanoparticles in the presence of impurity and seed crystal. Induction time measurement was carried out at three temperatures, 298, 308 and 318 K. Four reproducible experiments were carried out in each run. Absorption of solution at 410 nm was recorded at different times on a Varian Cary 50 Conc spectrophotometer to measure induction time. As Fig. 1 shows, a graph of absorption vs. time is plotted and the time of rise in absorption is taken as the induction time.

4. Results and discussion

In this study, utilizing the results of the experiments; the authors interpreted the effects of supersaturation, temperature, Fe^{3+} impurity and crystal seed on the induction time of silver nanoparticles using two models, Smoluchowski's coagulation theory and cluster coagulation model. The results were also compared with experimental ones to find the most suitable model.

4.1. Effect of supersaturation and temperature on induction time

Table 1 shows the experimental data of induction time for the seeded and unseeded case. According to the

Fig. 1. Absorption of solution at different times for precipitation of silver nanoparticles at $S = 1 \times 10^8$ and T = 298 K.

experimental data in Table 1, the decrease in induction time at higher supersaturation is mainly caused by the higher coagulation concentration of clusters and the smaller critical nuclei size, and also the decrease in induction time at higher solution temperature is caused by the smaller interfacial energy of crystal at higher solution temperature.
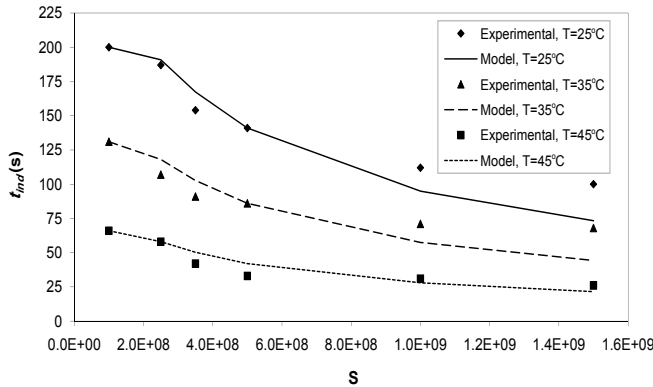
Based on Smoluchowski's coagulation theory (Eqs. (7a) - (7c)), The following values are used to calculate the induction time: k=1.3805×10^{-23} J/K and V_m =1.70728×10^{-29} m^3. The saturation concentration of silver in the solution is 2×10^{-12} M [13]. The initial values of silver nitrate concentration corresponds to supersaturation: $S = \dfrac{C}{C^*} = 10^8$ to 15×10^8. C^* denotes saturation concentration. The value of the association coefficient between two clusters $K_{i = 1,2,3}$ in Eqs. (7a)-(7c) and interfacial tension, δ, is estimated by fitting the models to the experimental data of induction time by minimizing the total absolute deviation, ε, defined as

$$\varepsilon = \frac{\sum \left| t_{ind,exp} - t_{ind,mod} \right|}{t_{ind,exp}}$$. The subscript *exp* and *mod*

indicate experimental and model, respectively. Values of t_{ind} calculated by the first model at T=298 K are summarized in Table 2.

After determining K_i and δ for each temperature, it was found that the model based on Eq. (7c) predicts the experimental induction times much better. In the other words, the rate of formation of clusters is independent of their size and relates to the product of the sizes of their precursors. Fig. 2 compares the theoretical induction time calculated by Eq. (7c) with experimental data at three temperatures. Fig. 2 shows that the calculated induction times are in good agreement with the experimental data.

The following values are used in Eq. (14) to calculate the induction time: η = 8.93×10^{-4}, 7.21×10^{-4} and 5.95×10^{-4} N.s/m^2 for T = 298, 308 and 318 K,

Table 1. Experimental induction time in seconds at different temperatures and supersaturation for seeded and unseeded case.

Temperature (K)		Supersaturation					
		1×10^8	2.5×10^8	3.5×10^8	5×10^8	10×10^8	15×10^8
298	without seed	200	187	154	141	112	100
	with seed	112	86	62	60	56	41
308	without seed	131	107	91	86	71	68
	with seed	65	50	45	43	39	28
318	without seed	66	58	42	33	31	26
	with seed	47	37	35	27	25	24

Fig. 2. Variation of experimental induction time by theoretical data calculated by Smoluchowski's coagulation theory.

respectively. $\bar{g}$ and δ are estimated by minimizing the error ε between model and experimental data and are shown in Table 3 for T = 298 K.

Here, the interfacial tension and the viscosity of solution in the supersaturation range investigated are assumed to be constant because of the very low solubility of silver. It is found that the total absolute deviation has the smallest value when $\bar{g}$ =1 and δ =473.8 mJ/m^2 at T =298 K, $\bar{g}$ =1 and δ =487.6 mJ/m^2 at 308 K, and $\bar{g}$ =1 and δ =497.9 mJ/m^2 at 318 K. The results imply that the monomer is a dominant size of clusters existing in the supersaturated solution to form nuclei.

As Fig. 3 shows, results of the cluster coagulation model are very different from the experimental data indicating that the actual process is different and cannot be interpreted by the second theoretical model. In other words, the Smoluchowski model is based upon monomer coagulation and the cluster model is based upon g-mer (g could be any number) doubling. With no strings attached, one would naturally expect the conventional Smoluchowski model describes a process that is closer to reality, whereas the cluster model may only be an extreme case if it is realistic at all. In other words, it is truer to conclude that the cluster model is overly simplified and does not properly depict the precipitation process.

4.2. Effect of impurity on induction time

The effect of soluble impurities may be caused by changing the equilibrium solubility or the solution structure, by adsorption or chemisorption on the nuclei or hetronuclei, by chemical reaction or complex formation in the solution, and so on [1]. Chemical affinity and chemical potential between the inhibitor anion and crystal-positive ion have an important influence on the adsorption of the complex on the surface of the molecules and crystal [14].
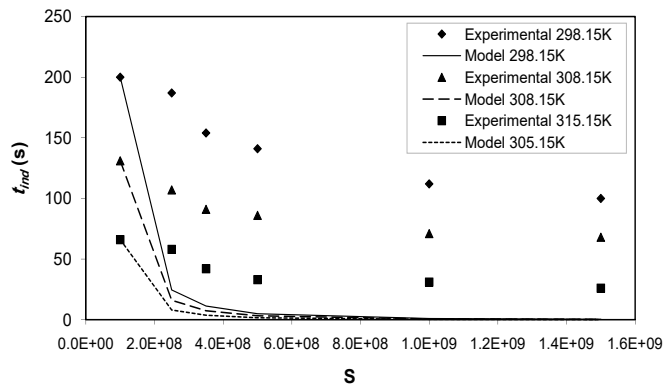
Fig. 3. Variation in the induction time as a function of supersaturation calculated by cluster coagulation theory at various solution temperatures.

Table 2. Comparison of measured and predicted induction time (in seconds) by Smoluchowski's coagulation theory for three different association mechanisms at T = 298 K.

S	Time, exp. (sec)	Based on Eq. (7a)	Based on Eq. (7b)	Based on Eq. (7c)
		$K_1 = 0.004$	$K_2 = 0.0025$	$K_3 = 0.0064$
1×10^8	200	199.97	200	200
2.5×10^8	187	203.20	197.05	190.85
3.5×10^8	154	173.46	170.46	167.35
5×10^8	141	141	140.98	141
10×10^8	112	87.65	90.99	94.92
15×10^8	100	64.44	68.45	73.32
ε		0.786	0.664	0.527

at T = 298 K: ε = 0.526, δ = 340.8 mJ/m^2, K_3 = 0.0064 m^3/mol.s
at T = 308 K: ε = 0.771, δ = 350.6 mJ/m^2, K_3 = 0.0109 m^3/mol.s
at T = 318 K: ε = 0.741, δ = 361.2 mJ/m^2, K_3 = 0.0228 m^3/mol.s

The experimental values of induction time obtained at five levels of impurity (Fe^{3+}) concentrations and for three levels of temperatures are summarized in Table 4. We consider the interfacial tension and association coefficient as a function of concentration ratio of $[Fe^{3+}]/[Ag^+]$ at each level of temperatures. Therefore, we attempted to estimate interfacial tension and association coefficient using Smoluchowski's coagulation theory (based on Eq. (7c)). Table 5 shows the analysis results of interfacial tension and association coefficient of silver nanoparticles.

Estimated values are summarized in Table 6. The theoretical induction times were predicted by Eq. (7c) based on Smoluchowski's coagulation theory. As can be seen from Fig. 4, there is good agreement between experimental and theoretical values of induction time in the presence of impurity at each level of temperatures. The results show that the presence of Fe^{3+} prolongs the induction time by increasing the interfacial tension and decreasing the association coefficient.

According to previous analysis, we substituted $\bar{g} = 1$ and an equation for interfacial tension in Eq. (14) and predicted the impurity's effect on induction time of silver nanoparticles by the cluster coagulation model. Table 7 shows the analysis results of interfacial tension
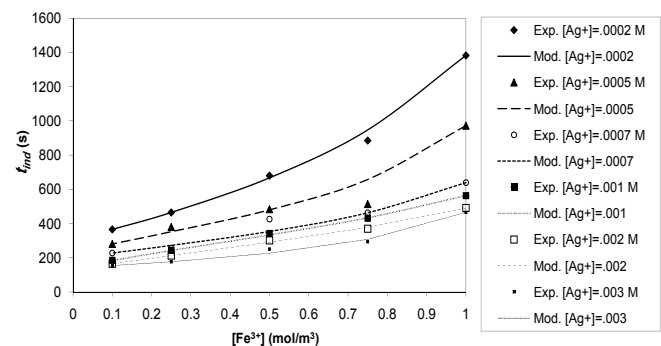
Fig. 4. Variation in the induction time as a function of impurity concentration calculated by Smoluchowski's coagulation theory at T = 298 K.

of silver nanoparticles at each level of temperatures. The proper values of *a* and *b* are summarized in Table 8. Crystal-positive ion have an important influence on the adsorption of the complex on the surface of the molecules and crystal [14].

Fig. 5 shows the experimental and theoretical value of induction time against Fe^{3+} concentration. The theoretical induction times were predicted by Eq. (14) based on the cluster coagulation model. It appears that the cluster coagulation model is a good model for recalculating the induction time of the silver nanoparticles solution in the presence of Fe^{3+}.

Table 3. A comparison of calculated ε for various $\bar{g}$ by cluster coagulation model at T = 298 K.

S	t_{ind},exp (sec)	Calculated induction times based on Eq.(14) (sec)			
		$\bar{g} = 1$	$\bar{g} = 2$	$\bar{g} = 3$	$\bar{g} = 4$
1×10^8	200	199.99	199.99	199.99	199.99
2.5×10^8	187	24.53	1.74	7.26	2.47
3.5×10^8	154	11.29	2.34	2.07	0.48
5×10^8	141	4.94	1.38	0.54	0.09
10×10^8	112	0.97	0.29	0.04	0.003
15×10^8	100	0.37	0.11	0.01	0.0004
ε		4.748	4.962	4.943	4.983

Table 4. Experimental induction time in seconds at presence of impurity at different temperatures and supersaturation.

S	Impurity Concentration (M)														
	1×10^{-3}			0.75×10^{-3}			0.5×10^{-3}			0.25×10^{-3}			1×10^{-4}		
	298K	308K	318K	298K	308K	318K	298K	308K	318K	298K	308K	318K	298K	308K	318K
1×10^8	1382	484	277	885	422	265	680	319	190	465	232	182	366	182	148
2.5×10^8	972	253	116	514	219	105	484	190	100	380	157	72	281	147	71
3.5×10^8	639	211	100	463	168	95	426	150	77	256	145	66	228	142	43
5×10^8	563	172	97	431	142	84	342	117	65	243	105	62	185	102	35
10×10^8	491	158	82	370	123	78	302	108	64	213	94	60	165	80	33
15×10^8	466	115	77	294	101	67	251	80	61	177	72	54	155	69	32

Table 5. Interfacial tension and association coefficient estimated by Smoluchowski's coagulation theory.

Temperature (K)	Interfacial tension (J/m^2)	Association coefficient $(m^3/mol.s)$
298	$\delta = 0.340773(a+b\frac{[Fe^{3+}]}{[Ag^+]})$	$K_3 = 0.006378(a'+b'\frac{[Fe^{3+}]}{[Ag^+]})$
308	$\delta = 0.350604(a+b\frac{[Fe^{3+}]}{[Ag^+]})$	$K_3 = 0.01093(a'+b'\frac{[Fe^{3+}]}{[Ag^+]})$
318	$\delta = 0.361178(a+b\frac{[Fe^{3+}]}{[Ag^+]})$	$K_3 = 0.022836(a'+b'\frac{[Fe^{3+}]}{[Ag^+]})$

Table 6. Fitting parameters a, b, a' and b' in interfacial tension and association coefficient expressions by Smoluchowski's coagulation theory at each level of supersaturation.

S	T (K)	a	b	a'	b'	ε
1×10^8	298	1.15	0.03	1.32	-0.15	0.089
	308	1.13	0.05	1.33	-0.06	0.061
	318	1.28	1.04	2.47	-0.18	0.206
2.5×10^8	298	1.43	0.67	1.68	-0.54	0.36
	308	1.54	0.21	1.83	-0.3	0.044
	318	1.53	1.53	1.9	-0.23	0.186
3.5×10^8	298	1.56	0.92	1.6	-0.65	0.235
	308	0.82	0.07	1.98	-0.97	0.015
	318	1.03	1.03	1.72	-0.23	0.096
5×10^8	298	1.25	0.84	0.93	-0.45	0.031
	308	2.24	0.28	1.78	-0.79	0.085
	318	0.64	0.64	1.44	-0.54	0.137
10×10^8	298	1.26	1.48	0.52	-0.49	0.059
	308	2.28	1.92	1.04	-0.97	0.119
	318	0.63	0.63	0.71	-0.36	0.114
15×10^8	298	1.75	1.08	0.58	-1.15	0.144
	308	2.44	1.99	0.89	-1.13	0.113
	318	0.44	0.44	0.57	-0.56	0.035

Table 7. Interfacial tension estimated by cluster coagulation model.

| Temperature (K)	Interfacial tension (J/m^2)
298	$\delta = 0.473789(a+b\frac{[Fe^{3+}]}{[Ag^+]})$
308	$\delta = 0.487631(a+b\frac{[Fe^{3+}]}{[Ag^+]})$
318	$\delta = 0.497932(a+b\frac{[Fe^{3+}]}{[Ag^+]})$

Table 8. Fitting parameters a and b in interfacial tension expressions by cluster coagulation model at each level of supersaturation.

S	T (K)	a	b	ε
1×10^8	298	1.01	0.007	0.124
	308	1.01	0.006	0.258
	318	1.14	0.05	0.248
2.5×10^8	298	1.05	0.016	0.435
	308	1.05	0.007	0.046
	318	1.05	0.007	0.223
3.5×10^8	298	1.07	0.019	0.249
	308	1.07	0.005	0.207
	318	1.06	0.013	0.502
5×10^8	298	1.08	0.028	0.184
	308	1.08	0.015	0.144
	318	1.08	0.024	0.538
10×10^8	298	1.12	0.054	0.165
	308	1.11	0.036	0.113
	318	1.11	0.04	0.699
15×10^8	298	1.14	0.09	0.221
	308	1.13	0.042	0.135
	318	1.14	0.05	0.565

4.3. Effect of crystal seed on induction time

The experimental results in Table 1 indicate that the induction times of seeded cases are shorter than unseeded cases. This decrease can be explained by an increase in the concentration of clusters near the crystal surface, this also implies that the van der Waals attraction force between cluster and crystal seed plays an important role in the formation of critical nuclei of silver in the secondary nucleation regime [7,15].

Here, we assume that the association coefficient of clusters, interfacial tension, and $\bar{g}$ in the seeded case, are the same as the unseeded case. Hamaker constant,
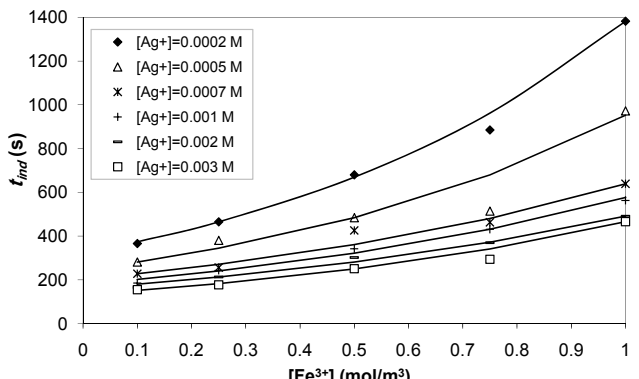
Fig. 5. Variation in the induction time as a function of impurity concentration calculated by cluster coagulation model at T = 298 K.

A, is about 6×10^{-20} J for silver and we assume that the value of A for silver nitrate is like silver, and the radius of the spherical silver atom r_1 is 1.6×10^{-10} m.

Fig. 6 compares the experimental induction time in the seeded case at T = 298 K, with the theoretical induction time calculated by the cluster coagulation model and Smoluchowski's coagulation theory. As can be seen, Smoluchowski's coagulation theory is much better than the cluster coagulation model in reproducing results.

Calculating ε, shows $d = 4.8\times10^{-10}$ m for Smoluchowski's coagulation theory. So, nucleation occurs at this distance from the surface of the seed crystal, which is about 1.5 times of silver monomers' radius.
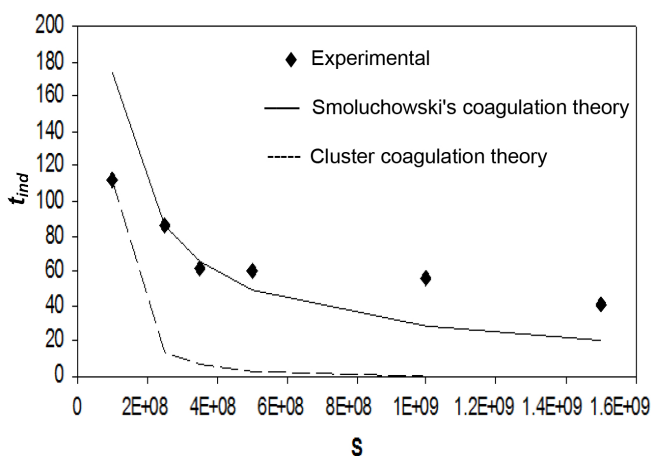
4.4. Comparison of interpreting models for induction time

We can use the average absolute deviation (*AAD*) as a comparison measure to determine the appropriate model for predicting the induction time of silver nanoparticles,. The *AAD* is calculated by:

$$\%AAD = \frac{1}{N_P}\sum\left|\frac{A_{exp.} - A_{mod.}}{A_{exp.}}\right|\times100 \qquad (22)$$

where N_P is the number of data obtained by fitting analysis. Final results for precipitation of silver nanoparticles, addition of impurity and crystal seed are summarized in Table 9.

According to Table 9, in the all cases, minimum calculated values of *AAD* were attained by Smoluchowski's coagulation theory. Therefore, Smoluchowski's coagulation theory is the best prediction model for precipitation of silver nanoparticles.

5. Conclusions

Silver nanoparticles are produced by precipitation, and the induction time is measured at different temperatures and supersaturation. As it can be seen from the experimental data, the induction time decreases with increasing supersaturation and temperature. Crystal seeds reduce the induction time while the inverse effect can be seen in the presence of Fe^{3+}. The increase in the induction time when Fe^{3+} is present may be caused by an increase in the interfacial energy. The effects of impurity and seed crystal on the induction time of silver nanoparticles were theoretically studied by employing Smoluchowski's coagulation theory and cluster coagulation model. The analysis of models showed that the Smoluchowski's coagulation theory is more suitable.

References

[1] W. Beckmann, Crystallization: Basic Concepts and Industrial Applications, Wiley-VCH; 2013.

[2] S. Prabhu, E.K. Poulose, Silver nanoparticles: Mechanism of antimicrobial action, synthesis, medical applications, and toxicity effects, Int. Nano Lett. 2 (2012) 32-36.

Fig. 6. A comparison of calculated induction time of seed case by Smoluchowski's coagulation theory and cluster coagulation model at T = 298 K.

Table 9. Results of average absolute deviation for prediction models of induction time at three cases: precipitation silver nanoparticles, presence of impurity and addition of crystal seed.

		T (K)	Model	N_P	*%AAD*
Smoluchowski's coagulation theory	Without seed	298-318	7c	18	11.33
	With seed	298-318	9c	18	21.99
	Impurity	298-318	7c	90	2.41
Cluster coagulation model	Without seed	298-318	14	18	78.77
	With seed	298-318	17	18	78.65
	Impurity	298-318	14	90	5.62

[3] P.E.J. Saloga, C. Kästner, A.F. Thünemann, High-speed but not magic: Microwave-assisted synthesis of ultra-small silver nanoparticles, Langmuir, 34 (2018) 147-153.

[4] Ö. Karhan, Ö.B. Ceran, O.N. Şara, B. Şimşek, Response surface methodology based desirability function approach to investigate optimal mixture ratio of silver nanoparticles synthesis process, Ind. Eng. Chem. Res. 56 (2017) 8180-8189.

[5] X.-W. Han, X.-Zh. Meng , J. Zhang, Ji.-X. Wang, H.-F. Huang, X.-F.,Zeng, J.-F. Chen, Ultrafast synthesis of silver nanoparticle decorated graphene oxide by a rotating packed bed reactor, Ind. Eng. Chem. Res. 55 (2016) 11622-11630.

[6] G. Zhang, Y. Liu, X. Gao, Y. Chen, Synthesis of silver nanoparticles and antibacterial property of silk fabrics treated by silver nanoparticles, Nanoscale Res. Lett. 9 (2014) 216-220.

[7] C.Y. Tai, W.C. Chein, J.P. Hsu, Induction period of $CaCO_3$ interpreted by the Smoluchowski's coagulation theory, AIChE J. 51 (2005) 480-486.

[8] R.Y. Qian, G.D. Botsaris, A new mechanism for nuclei formation in suspension crystallizers: the role of interparticle forces, Chem. Eng. Sci. 52 (1997) 3429-3440.

[9] S. Das, J. Das, A. Samadder, S.S. Bhattacharyya, D. Das, A.R. Khuda-Bukhsh, Biosynthesized silver nanoparticles by ethanolic extracts of Phytolacca decandra, Gelsemium sempervirens, Hydrastis canadensis and Thuja occidentalis induce differential cytotoxicity through G2/M arrest in A375 cells, Colloid Surface B, 101 (2013) 325-336.

[10] C.Y. Tai, W.C. Chein, Interpreting the effects of operating variables on the induction period of $CaCl_2$-Na_2CO_3 system by a cluster coagulation model, J. Chem. Eng. Sci., 58, (2003), 3233-3241.

[11] H. Zhang, J.A. Smith, V. Oyanedel-Craver, The effect of natural water conditions on the anti-bacterial performance and stability of silver nanoparticles capped with different polymers, Water Res. 146 (2012) 691-699.

[12] P. Mulvaney, Surface Plasmon Spectroscopy of Nanosized Metal Particles, Langmuir, 12 (1996) 788-800.

[13] L. Sintubin, W. De-Windt, J. Dick, J. Mast, D. van der Ha, W. Verstraete, N. Boon, Lactic acid bacteria as reducing and capping agent for the fast and efficient production of silver nanoparticles, Appl. Microbiol. Biot. 84 (2009) 741-749.

[14] M.M. Reddy, A. Hoch, Calcite Crystal Growth Rate Inhibition by Polycarboxylic Acids, J. Colloid Interf. Sci. 235 (2001) 365-370.

[15] K.V. Rajendran, R. Rajasekaran, D. Jayarman, Experimental determination of metastable zonewidth, induction period, interfacial energy and growth of non-linear optical l-HFB single crystals, Mater. Chem. Phys. 81 (2002) 50-55.